What are the true values of the bending modulus of simple lipid bilayers?

John F. Nagle[*], **Michael S. Jablin**, **Stephanie Tristram-Nagle**, and **Kiyotaka Akabori**
Department of Physics, Carnegie Mellon University, Pittsburgh, PA 15213 USA

Abstract

Values of the bending modulus K_C are reviewed, and possible causes for the considerable differences are discussed. One possible cause is the use of glucose and sucrose in the classical micromechanical manipulation and shape analysis methods. New data, using the more recent low angle x-ray method, are presented that do not support an effect of glucose or sucrose on K_C. Another possible cause is using an incomplete theory to interpret the data. Adding a tilt term to the theory clearly does not affect the value obtained from the shape analysis method. It is shown that a tilt term, using a value of the modulus K_θ indicated by simulations, theory, and estimated from order parameters obtained from NMR and from the wide angle x-ray method, should also not affect the value obtained using the micromechanical manipulation method, although it does require a small correction when determining the value of the area compressibility modulus K_A. It is still being studied whether including a tilt term will significantly affect the values of K_C obtained using low angle x-ray data. It remains unclear what causes the differences in the experimental values of K_C for simple lipid bilayers.

Keywords

Membrane mechanics; bending modulus; area compressibility modulus; tilt modulus; lipid bilayers; DOPC

1. Introduction

The bending modulus K_C is a most important membrane mechanical property. Accordingly, it has been measured many times for many different lipid bilayers. Although uncertainties are typically reported at the 10% level, values obtained in different labs and with different measuring techniques typically differ by as much as a factor of two for the same lipid at the same temperature (Nagle, 2013, Marsh, 2006). As biological processes often involve transition states with curved membranes, that part of the activation energy would differ by a factor of two. For thermally activated processes, the predicted rate constant, depending as it

[*]Corresponding author nagle@cmu.edu and 412-268-2764.

does on the exponential of the activation energy, could easily be kinetically incompetent for the larger K_C value, while being quite feasible for the smaller value (Nagle, 2013). It is therefore of some biophysical importance to obtain more accurate values of K_C, as well as to alleviate the embarrassment that membrane researchers lack accepted values for a quantity that is recognized to be central.

The two most common methods for measuring K_C are micromechanical manipulation (MM) of giant unilamellar vesicles (GUV) (Rawicz et al., 2000, Henriksen and Ipsen, 2004, Vitkova et al., 2006, Shchelokovskyy et al., 2011, Evans and Rawicz, 1990), often called the pipette aspiration method, and fluctuating shape analysis (SA) of GUV (Meleard et al., 1998, Henriksen and Ipsen, 2002, Meleard et al., 1997, Pecreaux et al., 2004, Gracia et al., 2010) and many earlier references (Bouvrais, 2012, Vitkova and Petrov, 2013). A few results have been obtained by pulling cylindrical tethers from GUV (Heinrich and Waugh, 1996, Sorre et al., 2009, Tian et al., 2009) and a variety of other techniques are reviewed by (Dimova, 2014). Here we will focus on some MM and SA results as well as results from an x-ray method. Analysis of low angle diffuse x-ray scattering from oriented stacks of membranes has also been employed more recently (Lyatskaya et al., 2001, Liu and Nagle, 2004, Salditt et al., 2003, Li et al., 2006, Pan et al., 2008, Pan et al., 2009), and the values so obtained agree well with those reported in a classic MM paper (Rawicz et al., 2000). However, ignoring for the moment differences between different labs using the same method, the values obtained using SA are generally larger than those obtained using MM or x-ray methods (Nagle, 2013, Marsh, 2006). One possible reason may be related to different length scales of the measurements and the theory involved, as we review in Section IV. A more mundane possibility regards an experimental aspect of the two GUV methods to which we first turn in the next section.

2. What is the effect of sugar concentration c_s on the bending modulus?

The MM method typically uses a sugar solution to conserve the volume of the GUV (Vitkova et al., 2006, Evans and Rawicz, 1990). Often a sucrose solution inside the GUV and a glucose solution outside the GUV is used to enhance visual contrast. A classic study used $c_s = 200$mM sugar with the same molarity on both sides to ensure flaccid GUV with zero imposed surface tension or pressure; Fig. 1 shows the reported value (red right pointing triangle) of K_C/kT for DOPC, that has two double bonds in the two oleoyl (DO) hydrocarbon chains, and the value (blue right pointing triangle) for SOPC, that has a saturated stearoyl (S) chain that makes the SOPC bilayer a bit thicker and stiffer than DOPC (Rawicz et al., 2000). Also shown in Fig. 1 are the results from the first study that reported an effect of sugar concentration on SOPC (Vitkova et al., 2006). This study utilized the SA method for small sucrose concentrations (two open blue down triangles in Fig. 1) and the MM method (four solid down blue triangles in Fig. 1) for larger sucrose concentrations (fluorescent dye was used for contrast instead of glucose outside). These results, when interpolated at 200mM, are about a factor of two smaller than the earlier results (Rawicz et al., 2000), perhaps attributable to differences in the way the two labs interpreted MM data. More importantly, an exponential decay with sugar concentration was indicated, as shown by the lower dashed blue line in Fig. 1. The same group, using the SA method exclusively, also reported a decreasing K_C with increasing sucrose concentration, although the decrease

was only about half as large as in Fig. 1 (Genova et al., 2006). Subsequently, decreasing K_C was reported for other sugars (Genova et al., 2007), although, contrarily, maltose was reported not to decrease K_C (Genova et al., 2010). Figure 1 also shows the most recent SOPC value (open square) with no sugar obtained after further development of the SA method (Genova et al., 2013).

An MM study of DOPC found that K_C at small c_s = 8mM sucrose/8mM glucose was twice as large as with 100mM sucrose/110 mM glucose (Shchelokovskyy et al., 2011). As shown by the red dashed line in Fig. 1, that is also consistent with a strong exponential decay with sugar concentration; extrapolation to 200mM gives a value three times smaller than the earlier DOPC result of (Rawicz et al., 2000). Interestingly, the same exponential dependence connects the earlier MM value for SOPC of (Rawicz et al., 2000) with the values of K_C reported by (Henriksen and Ipsen, 2004) using the MM method and by (Henriksen and Ipsen, 2002) using the SA method (half closed squares in Fig. 1). Finally, Fig. 1 shows that our x-ray results at zero sugar (upright triangles) agree well with the earlier MM results (right pointing triangles).

Not surprisingly, considering the current state of K_C results, there is the feeling that more experiments should be done (Genova et al., 2013) (Dimova, 2014). However, instead of only exhorting others to do more experiments, we have been addressing this issue using the x-ray method.

3. New x-ray results for possible sugar effect

Briefly, four samples (i–iv) were made by mixing DOPC and sugar (first solubilized in heated trifluoroethanol or methanol) in excess 1:1 chloroform/(trifluoroethanol or methanol) organic solvent with mole ratios of (i) 0.12 glucose/DOPC, (ii) 0.12 sucrose/DOPC, (iii) and (iv) 0.22 glucose/DOPC. The mixtures were deposited on Si wafers using the rock and roll technique to achieve superior alignment in the stack of about 2000 bilayers (Tristram-Nagle, 2007). The dry sample was then hydrated in a humidity chamber in situ on the x-ray beamline. Hydration was conveniently even more rapid with sugar than for pure DOPC. Compared to the repeat spacing of fully hydrated DOPC, D=63.1 Å, the repeat spacing increased to D ≈ 68 Å for the lower concentrations in samples (i) and (ii), and for the higher concentrations in samples (iii) and (iv) D increased to 74 Å. Fig. 2 shows a grayscale image of the x-ray scattering. K_C/kT was obtained using our analysis procedure (Liu, 2003).

New x-ray results are shown in Fig. 3 along with some of the literature results already shown in Fig. 1. In order to facilitate comparison between various results, K_C has been normalized to 1 for zero sugar, except for the MM result for DOPC at 200mM for which the x-ray result was used for the normalization. The x-ray K_C result with no sugar has been shifted to a slightly negative concentration to allow it to be seen distinctly from the SOPC result; the small x-ray uncertainty is the estimated uncertainty in the mean obtained from 27 DOPC samples studied over a period of ten years. The standard deviation for the distribution of K_C for these 27 samples is 5.2 times larger, and that is the assumed uncertainty shown by the error bars for the new data. However, we emphasize that for samples (iii) and (iv), several D spacings were achieved for the same sample by systematically varying the relative

humidity. This gave a range of sugar concentrations for the same sample, so the same uncertainty applies to all the K_C values for that sample. That is to say, K_C for all the concentrations has an uncertainty given by the error bar, but the concentration dependence shown by the slope of the line is not affected by this uncertainty. As that slope is essentially zero, samples (iii) and (iv) show negligible dependence of K_C on glucose concentration. More importantly, the values for each of those samples are remarkably close to the average value for the 27 samples with no sugar.

The amount of sugar added in samples (i) and (ii) was designed to correspond to 200mM sugar in fully hydrated DOPC, calculated from the result that DOPC has $n_W=30$ water molecules/lipid between the bilayers with lamellar repeat spacing D=63.1 Å (Nagle and Tristram-Nagle, 2000, Kucerka et al., 2008) and area A = 67.4 Å^2 (Kucerka et al., 2008). There are two reasons that the concentrations displayed in Fig. 3 for samples (i) and (ii) are smaller. The first reason is that the repeat spacing was larger, D = 68 Å, for both glucose (i) and sucrose (ii). As the bilayer dimensions changed very little, n_w should be increased to 35.5, decreasing these nominal sugar concentrations to 164 mM.

The effective sugar concentration can be further reduced if there is binding of sugar molecules to the lipid, over and above the number of sugars per lipid that would dissolve in the n_w intercalated waters. If such binding occurs, then the number n_s of sugars/lipid, which is $n_s=0.11$ from the weights of sugar and lipid in samples (i) and (ii), is the sum of bound, n_{sb}, and unbound, n_{sub}, sugars, and the concentration that must be compared to MM and SA experiments is the nominal concentration of 164mM times n_{sub}/n_s. Whether there is net binding or the opposite, net exclusion, has been controversial, with recent work (Andersen et al., 2011) concluding that there is net binding for small concentrations and net exclusion for larger concentrations. Using the data in Fig. 3 of (Andersen et al., 2011), we estimate that $n_{sub}/n_s \sim 0.64$ for samples (i) and (ii), which multiplied by 164mM gives 105mM; this is the concentration shown in Fig. 3 for those samples. However, for our higher concentrations, the same figure indicates no net binding or exclusion, so no n_{sub}/n_s factor was applied to the concentrations of samples (iii) and (iv).

There is yet another consideration that could reduce the effective sugar concentration. During the evaporation of the organic solvent used to mix lipid and sugar, a fraction f of the sugar could have accumulated into defect regions free of lipid instead of being intercalated between the dry oriented bilayers. Assuming that this sugar did not migrate when the sample was hydrated would decrease the number of sugars between adjacent bilayers to $(1-f)n_s$. Nevertheless, it is clear that some sugar resided between the bilayers because the fully hydrated D spacing increased when sugar was added. (In passing, note that the value of the D spacing reflects a balance mostly between the attractive van der Waals interaction and the repulsive fluctuation pressure, the hydration force being small near full hydration. As the fluctuation pressure depends on K_C, and that value did not change with sugar, the total sugar, intercalated plus bound, likely reduces the van der Waals attraction.) In the extreme case, if sugar had been totally excluded from between the bilayers, then hydration would have formed pools of sugar/water in contact with the stack of bilayers. Such pools would have exerted an osmotic stress on the water between the bilayers, sucking it out and thereby reducing D compared to that of fully hydrated bilayers with no sugar, rather than increasing

D as observed. For the relevant case of a fraction (1-f) of the sugar present between the bilayers and f excluded, then upon hydration, as water is more permeable by four orders of magnitude than sugar, water would enter both between the bilayers and into the pools, resulting in equal sugar concentrations in both locations. Then the total volume of the pools would be f/(1-f) times the volume of the water between the bilayers; the latter volume is 45% of the volume of the DOPC bilayer stacks when D=68Å and A=67.4Å^2 (Kucerka et al., 2008). We estimate that f=1/2 is an upper bound because it is likely that even this much volume of defect pools would disorient the sample, but no difference in mosaic spread was observed when sugar was added. (It might also be noted that the presence of defect pools impacted the Luzzati gravimetric method for measuring area/lipid, (Nagle and Tristram-Nagle, 2000, Koenig et al., 1997) with about 20% of the water in such pools for DOPC at full hydration. A difference is that the relative size of the pools to the intercalated water could be shrunk by applying osmotic pressure with a polymer, but here that ratio remains constant.)

Although we can only say that the sugar concentrations c_s for the x-ray results shown in Fig. 3 are upper bounds, we estimate that an additional reduction in the effective concentration c_s by even a factor of 2 is unlikely. Therefore, our new results do not support a dependence of K_C on sugar concentration. However, after initial submission of this paper, we noticed a recent result, included only in a book chapter, consistent with our result in Fig. 3 that glucose has a negligible effect on K_C. Contrary to (Genova et al., 2007), (Vitkova and Petrov, 2013) reported that glucose negligibly decreases K_C in eggPC bilayers, whereas sucrose continued to have an effect similar in magnitude to that reported for SOPC bilayers (Genova et al., 2006). Our result for sucrose at a single concentration in Fig. 3, while not indicating an effect on K_C, could be consistent with one. We plan to extend our sucrose studies to higher concentrations.

4. What is actually measured by the various techniques?

4.1. Standard Theory

The SA, MM and x-ray methods all measure time averaged displacements of the bilayer from the flat condition. If the flat bilayer is positioned in the $\mathbf{r}$ = (x,y) plane with z=0, then thermal fluctuations produce out-of-plane deviations z(x,y) that time average to zero, <z>=0, but that have non-zero mean square values <z^2> 0. It is assumed that the local energy of bending symmetric bilayers to positions z(x,y)=z(r) is given by

$$E_{bend}(\mathbf{r}) = (K_C/2)(\partial^2 z/\partial x^2 + \partial^2 z/\partial y^2)^2 \equiv (K_C/2)C(\mathbf{r})^2, \quad (1)$$

where C($\mathbf{r}$) is the local curvature. (Helfrich, 1973) Straightforward statistical mechanics enables calculation of the quantities of interest by Fourier transforming into reciprocal space with $\mathbf{q_r}$ = (q_x,q_y). This gives the well-known undulation spectrum

$$S(q_r) = \frac{kT}{K_C q_r^4 + \gamma q_r^2} \quad (2)$$

for the mean square amplitudes of the modes with wavelength $2\pi/q_r$, where $q_r = |\mathbf{q_r}|$ and γ is the surface tension. The surface tension is identically zero for the x-ray method where no difference in osmotic pressure can be applied to different sides of the bilayersm whereas it is systematically varied in the MM method as aspiration pressure is changed. The SA method directly measures the amplitudes of the smallest q_r modes with the longest wavelengths ($\lambda = 2\pi/q_r$, typically of order 10μm), so surface tension is kept small to be able to obtain K_C.

The MM method measures changes in the projected area α of a GUV as γ is varied over a wide range. As is well known (Rawicz et al., 2000, Evans and Rawicz, 1990), there are two contributions to α. The obvious contribution is the expansion of a flat membrane given by $\alpha_A = \gamma/K_A$, where K_A is the area compressibility modulus which is typically 250–300mN/m (Evans et al., 2013). However, the largest initial increase in projected area when small γ is applied comes from reducing the area α_U that was hidden in the undulations; α_U is obtained by integrating $S(q_r)q_r^3 dq_r$ from the smallest q_m limited by the radius $R \approx 10$μm of the GUV to the largest $q_M \sim \pi/a$ where a is an intermolecular in-plane distance of order 8Å, so the integration range spans a little more than 4 orders of magnitude. When $\gamma = 0$, the integral is logarithmic, so each decade of length scales contributes equally to the area. The area pulled out from undulations is then

$$\Delta\alpha_u = \alpha_u(0) - \alpha_u(\gamma) = (kT/8\pi K_C)\ln(1+\gamma/K_C q_m^2) \quad (3)$$

in the γ range of interest.

The x-ray method requires pair correlation functions $\langle z_n(\mathbf{r})z_m(\mathbf{r'})\rangle$, not only between points in the same bilayer, but also points in different n and m bilayers, which takes some additional calculation (Lyatskaya et al., 2001); the major physical difference is that fluctuations in the spacing between neighboring bilayers means that fluctuations in the z direction and the corresponding q_z modes must also be considered. Also, $\gamma = 0$, so Eq. (2) becomes

$$S(q_r, q_z) = \frac{kT}{K_C q_r^4 + B q_z^2}, \quad (4)$$

where B is the interbilayer compressibility modulus. The interaction term $B q_z^2$ reduces the amplitude of the small q_r modes within the same bilayer, thereby reducing $\langle z_n(\mathbf{r})z_n(\mathbf{r'})\rangle$ for the larger $\mathbf{r-r'}$ length scales.

4.2. Refined theory

All three methods in the preceding paragraphs should provide the same value for K_C for the theory in Eq. (1). However, there is a more refined theory (Hamm and Kozlov, 2000) that adds to the bending energy in Eq. (1) a local free energy that depends on molecular tilt $\mathbf{t(r)}$ with respect to the local bilayer normal,

$$E_{tilt}(\mathbf{r}) = K_\theta |\mathbf{t(r)}|^2/2, \quad (5)$$

and it also redefines the curvature in Eq. (1) by the addition of $grad_r(\mathbf{t(r)})$. This theory has a spectrum (May et al., 2007)

$$S(q_r) = \frac{kT}{K_C q_r^4} + \frac{kT}{K_\theta q_r^2}. \quad (6)$$

Estimates of the tilt modulus K_θ of order 50mN/m will be discussed in Section V. Assuming this value here and a typical value of $K_C = 10^{-19}$ J = 24kT, the q_r^{-4} term dominates $S(q_r)$ at the large length scale, so the true K_C is obtained by the SA method. However, the second term in (6) becomes larger than the first term when q_r exceeds $q_\theta = (K_\theta/K_C)^{1/2} \approx 0.7$ nm^{-1}, corresponding to a tilt length scale $\xi_\theta \equiv 1/q_\theta \approx 1.4$ nm. From there down to the molecular length scale of 0.8 nm comprises part of the decade of largest q_r.

4.3. Refined theory - MM method

In order to quantify what the preceding theory implies for the MM method, it is necessary to consider the theory with surface tension γ. Just as for the derivation with no surface tension, one adds a term consisting of γ times the excess surface area. Following (May et al., 2007), this already results in the following rather more complicated expression

$$S(q_r) = \frac{kT(1 + K_C q_r^2/K_\theta)}{K_C(1 + \gamma/K_\theta)q_r^4 + \gamma q_r^2}. \quad (7)$$

In addition, it can be argued that applying surface tension reduces the energy for tilting, in which case K_θ in Eq. (7) would be replaced by $K_\theta - \gamma$ to first order in γ. Recently a formula has been published for a model with even more additional parameters than the tilt modulus (Watson et al., 2013); when the extra terms are eliminated and the surface tension is retained only to leading order, which make only small differences for the experimentally accessible range, that formula reduces to Eq. (7) with K_θ replaced by $K_\theta - \gamma$.

Starting from the modified Eq. (7), the same procedure as for the conventional theory in Eq. (2) then predicts the following result for the area pulled out from undulations in an MM measurement

$$\Delta \alpha_u(\gamma) = \frac{kT}{8\pi K_C} \left[\left(1 - \frac{\gamma}{K_\theta}\right)^2 \ln\left(1 + \frac{\gamma(1 - \gamma/K_\theta)}{K_C q_m^2}\right) + \frac{2\gamma}{K_\theta}\left(2 - \frac{\gamma}{K_\theta}\right) \ln\left(\frac{q_M}{q_m}\right) \right] \quad (8)$$

Plotting this in Fig. 4 shows that there is little difference in the predicted MM measurements for the theory with tilt compared to the conventional theory in the small tension regime where K_C can be obtained from the intial slope. For larger γ the theory with tilt has a larger α because there is an additional degree of freedom that gives rise to additional area α_u that is then pulled out with increasing γ. However, for small γ it is the pulling out of large length scale (small q_r) undulations that dominates α, giving the same form as the conventional theory in Eq. (3).

Fig. 5 emphasizes the large γ regime where $\alpha(\gamma)$ is dominated by the lateral area expansion $\alpha_A(\gamma) = \gamma/K_A$. However, even in the conventional case, the slope of the $\alpha(\gamma)$ curve is greater than $\alpha_A(\gamma)$ because $\alpha_U(\gamma)$ continues to increase as the undulations continue to be pulled out. Although a naïve approach to obtaining K_A would just fit the slope of $\alpha(\gamma)$ in the large tension regime in Fig. 5, the appropriate way is to subtract $\alpha_U(\gamma)$ first and then

one re-obtains the exact K_A which was set to 250mN/m. When the tilt term is added, Fig. 5 shows that $\alpha(\gamma)$ is greater for all γ because of the extra tilt degree of freedom. Importantly, the slope is also greater at large γ.

The first interesting question now is, how much would the apparent K_A value differ from the true value if one fits data, affected by a tilt degree of freedom, with the conventional model that has no tilt degree of freedom. For the example in Fig. 5, the fitted K_A is 233mN/m, 7% smaller than the exact 250mN/m. The second interesting question is, are the residual errors in this fit large enough to diagnose that the conventional theory is incorrect? The answer is no; the largest residual to the fit is only 0.0002 for the example in Fig. 5, not even large enough to see in these plots and far smaller than experimental uncertainty. In other words, the conventional theory is adequate to fit MM data, but MM data are not sufficient to detect the presence or absence of a tilt degree of freedom, at least for typical values of the moduli.

The preceding analysis shows that not including a tilt degree of freedom in the analysis of MM data still obtains the true value of K_C. Therefore, this does not account for the experimental differences compared to results obtained from the SA method. Importantly, the MM method can not provide experimental evidence for or against including the tilt degree of freedom in modern models of lipid bilayers. Furthermore, as the preceding analysis shows that the MM method underestimates K_A if there is a tilt degree of freedom, determination of K_A by the MM method would require a value of K_θ from other sources. However, the error of not including this term appears to be less than 10%. This point should nevertheless be kept in mind when evaluating K_A from simulations; a value smaller than the true value should be expected when evaluating K_A using $A(\partial\gamma/\partial A)_T$. Interestingly, a recent simulation obtained a smaller value of K_A (277±10 mN/m) using this method compared to the K_A (321±37 mN/m) obtained from the area fluctuations σ_A using the formula $2AkT/N\sigma_A^2$ (Braun et al., 2013).

4.4. Refined theory applied to SA and x-ray methods

In the SA method, individual GUV have non-zero surface tension. The method observes fluctuations for q less than about 1 μm^{-1}, so the surface tension has to be small, of order 10^{-4} mN/m in order for the spectrum in either Eq. (2) or (7) to depend measurably upon $K_C \approx 10^{-19}$J. For such small γ the ratio of $S(q)$ in Eq. (7) to $S(q)$ in Eq. (2) differs from 1 only by about 10^{-6}, so the SA analysis would give the same value for K_C regardless of tilt, and the method would also have no possibility of determining the tilt modulus K_θ.

The x-ray method could be different. To model the samples which consist of bilayer stacks, the interbilayer compressibility energy must be included. This gives a height-height spectrum similar to Eq. (7) with each factor there of γq_r^2 replaced by Bq_z^2,

$$S(q_r, q_z) = \frac{kT(1+K_C q_r^2/K_\theta)}{K_C q_r^4 + Bq_z^2(1+K_C q_r^2/K_\theta)}. \quad (9)$$

This is considerably more complicated than Eq. (4), and even for that conventional model the computation of x-ray intensities is non-trivial, because there are both in-plane q_r and out-of-plane q_z modes, and pair correlation functions, not just $S(q_r,q_z)$, are required. With the

extra complexity introduced by tilt in Eq. (9), data analysis becomes even more computationally difficult. Would such a development be useful, or would it, like the MM method, not make any significant difference? A difference compared to the MM method is that the undulations of bilayers in a stack are constrained by neighboring bilayers, and this reduces the amplitudes of the small q_r undulations preferentially as the wavelength exceeds the lateral correlation length $\xi \equiv (K_C/B)^{1/4} \approx 5$nm. This is comparable to the tilt length scale $\xi_\theta = (K_c/K_\theta)^{1/2} \approx 1.4$ nm below which tilt becomes dominant. Therefore, in contrast to MM data which are affected by four decades of length scales, the x-ray data are determined predominantly by the smallest decade, so it is more likely that tilt might affect the x-ray values of K_C. Another reason that incorporation of a tilt modulus into the x-ray data analysis could be valuable is that, with signal/noise becoming higher, small but systematic differences have been appearing between the fits and the data using the conventional theory, as shown in Fig. 2.

5. On obtaining values for the tilt modulus K_θ

Although the primary focus of this paper is on the bending modulus, the possible involvement of a tilt degree of freedom may make it of some interest to consider the value of its modulus in this section. A theoretical estimate of the tilt modulus gave $K_\theta \sim 100$mN/m (Hamm and Kozlov, 2000) and analysis of inverted hexagonal phase data led to $K_\theta \sim 80$mN/m (Hamm and Kozlov, 1998). (Note the factor of 2 is required to convert monolayer values to bilayers.) It is interesting that a model different from that of Hamm and Kozlov also provides a similar theoretical estimate for K_θ. This alternative model supposes that a tilted chain continues to have the same overall length and the same cross-sectional area perpendicular to its tilt axis, thereby requiring the interfacial area to increase by $A \sim t^2/2$ to conserve volume. The increase in hydrophobic free energy would then scale as $\gamma_{ow}t^2/2$ for each monolayer, where the oil-water surface tension $\gamma_{ow} \approx 50$mN/m would then be half the value of the tilt modulus for a bilayer. We note that this model motivated the replacement after Eq. (7) of K_θ by $K_\theta - \gamma$ because an applied surface tension γ decreases the interfacial free energy of tilting. This model differs from the original theory of Hamm and Kozlov which does not rescale K_θ upon tilting, instead maintaining the interfacial area and requiring the tilted chains to stretch in order to maintain constant volume. We have been informed by Evan Evans that a polymer brush model (Rawicz et al., 2000) also predicts the same value of K_θ and predicts that tilted chains stretch, unlike the alternative model above, but only 1/3 as much as the Hamm and Kozlov model. It would be of interest to examine simulations to evaluate these different models by correlating chain stretching with chain tilting, both of which are easily defined in simulations. It is interesting that all three models give the same value of K_θ.

Values ranging from 50–110mN/m have been reported from spectral analysis of coarse grained simulations (May et al., 2007, Watson et al., 2012). The most realistic simulation that had a large enough length scale for spectral analysis has been an atomistic simulation for DMPC (Brandt et al., 2011). When analyzed using a direct Fourier method, there appeared to be no q_r^{-2} term in the $S(q_r)$ spectrum, corresponding to infinite K_θ. However, analysis of the same simulation by imposing a real space envelope showed a q_r^{-2} term, consistent with $K_\theta = 56$mN/m (Watson et al., 2012); the difference between these two

methods of analysis is the subject of ongoing study (Albert et al., in preparation). A different simulation method that fitted the angular distribution to a potential of mean force obtained a monolayer $K_\theta \approx 6.7kT/A$ for DOPC (Khelashvili and Harries, 2013); for bilayers this is doubled to give 80 mN/m when A is approximated as 70 Å^2.

We next consider the use of chain order parameter data to estimate K_θ. The generic order parameter is defined as

$$S = (3<\cos^2\beta> - 1)/2, \quad (10)$$

where β is the angle away from the bilayer normal. Most commonly, deuterium NMR measures averages over the orientational distribution of individual CD bonds to obtain the S_{CD} order parameters as a function of carbon number. The value of S_{CD} in the plateau region can then be converted into the molecular order parameter $S_{NMR}=2|S_{CD}|$ (Seelig and Seelig, 1980). An order parameter S_{x-ray} has also been obtained from x-ray scattering in the wide angle range (Mills et al., 2008), distinct from the low angle x-ray scattering in Fig. 2 that has been considered so far. S_{x-ray} averages over the angular distribution of local bundles of tilted chains and is larger than S_{NMR} by about a factor of 1.4. In principle, S_{x-ray} might be more appropriate in that it addresses structure at the same length scale as the tilt parameter instead of at the level of individual methylene groups, but the differences do not substantially affect the following estimates of K_θ.

In terms of β, the absolute value of the tilt parameter **t** is tanβ which for small β can be approximated as sinβ. Therefore the total average chain tilt energy from Eq. (5) is

$$E_{tilt} \approx (K_\theta/2)<\sin^2\beta>(A_C N_C/2) = (K_\theta/2)A_C N_C(1 - S)/3, \quad (11)$$

where A_C is the mean area/chain and N_C is the total number of chains in both monolayers. Assuming independent tilt modes, as was assumed by (Khelashvili and Harries, 2013) and (May et al., 2004), equipartition of N_C chain tilt degrees of freedom then requires $E_{tilt} = N_C kT/2$. Combining with Eq. (10) then gives

$$K_\theta \approx 3kT/A_C(1 - S). \quad (12)$$

For DOPC at T=30° C, A_C=0.34nm^2, S_{x-ray} = 0.27 (Mills et al., 2008), yielding K_θ = 48mN/m. For DMPC at 30° C, A_C=0.30 nm^2, S_{x-ray}=0.40 (Pan et al., 2009), yielding K_θ = 70 mN/m. The simulated value of K_θ = 56 mN/m for united atom DMPC (Watson et al., 2012) is in reasonable agreement, but in the simulation the tilt parameter was defined for each lipid molecule rather than each chain; that replaces A_C in Eq. (12) with $A_L=2A_C$ which would reduce the order parameter estimate of K_θ to 35 mN/m. This raises the issue of what the basic unit, chains vs. molecules, should be for the tilt parameter.

Another issue is whether the basic unit, either chains or molecules, should be considered to be statistically independent. If tilt is correlated between chains, then the value of N_C in the assumption $E_{tilt} = N_C kT/2$ would be reduced and that would reduce K_θ. For the tilted DPPC gel phase, the correlation between chains persists to 2900 Å (Sun et al., 1994) indicating large numbers of chains in each independent unit. Of course, such long range persistence

does not occur in the disordered fluid phase where the width of the wide angle scattering indicates a lateral correlation length L that is only about 6 Å (Mills et al., 2008), thereby supporting nearly independent chains, although that L is the overall positional correlation length whereas the tilt-tilt correlation length could be larger. The tilt-tilt correlation length is an interesting quantity, one that could be determined by mining simulation data. Simulated tilt-tilt correlation lengths of cholesterol have been reported (Khelashvili and Harries, 2013) to be less than 1 nm and splay-splay correlation lengths of lipids have been reported to be less than 0.5 nm (Khelashvili et al., 2014 in press). Also, (May et al., 2004) suggest tilt-tilt correlations are negligible. Whatever reduction in N_C would be indicated, it is important to note that the assumption of independent modes gives an upper bound to K_θ and that the smaller the estimate for K_θ, the more important it is to include a tilt mode in the analysis of data and simulations.

It should also be noted that the experimental orientational order parameter S_{exp} is a product of the local tilt order parameter S_{tilt}, which is what should be used in Eq. (12), and an undulational order parameter S_{und} that accounts for undulations tilting the local bilayer normal from the laboratory z axis (Petersen and Chan, 1977). For small φ deviations, $S_{und} \approx 1 - 3\langle\varphi^2\rangle/4$. For the classical theory with no tilt, $\langle\varphi^2\rangle \approx 0.028$ giving $S_{und} \approx 0.98$ (Nagle and Tristram-Nagle, 2000). With tilt,

$$<\phi^2> \approx \frac{kT}{2\pi K_C}\left[\ln\left(\frac{\pi\xi}{a}\right) + \frac{1}{2}\left(\frac{\pi^2 K_C}{a^2 K_\theta}\right)\right] \quad (13)$$

where the x-ray analysis gives $\xi \approx 40$Å. The extra term on the right hand side would reduce S_{und} close to 0.9 using a=8 Å but a larger value of a closer to the bilayer thickness is probably more appropriate, returning S_{und} closer to 0.98. In either case, this appears to introduce only a secondary numerical correction to Eq. (12).

It is interesting to compare the estimate in Eq. (12) with the theoretical result $K_\theta=2\gamma_{ow}$ obtained at the beginning of this section. For both to be true, the interfacial hydrocarbon/water interaction, represented as γ_{ow}, would have to be larger for DMPC than for DOPC because S_{x-ray} is larger for DMPC. Nevertheless, it is encouraging that estimates from three theoretical models, from simulations, and from experimental order parameters give similar values of K_θ.

There is also a general issue that arises because there are two fundamentally different tilt moduli that are not necessarily equal. One is the theoretical modulus K_θ in Eq. (5) that is input into a statistical mechanical model. This is the modulus that is evaluated by fitting simulation data, using either the spectra such as those in Eqs. (6) and (7) or fitting the angular distribution to a potential of mean force (Khelashvili and Harries, 2013). The other modulus is the thermodynamic modulus, let us call it K_θ^+, that emerges from a statistical mechanical calculation of the model free energy. (Generally in statistical mechanics an input model parameter is not necessarily equal to a similarly named output thermodynamic quantity; the B modulus that appears in Eq. (9) is another example in membrane mechanics (Petrache et al., 1998).) For the thermodynamic modulus (May et al., 2004) calculated $K_\theta^+ = K_\theta + 3kT/A_C$ and both terms have similar magnitudes so their K_θ^+ is about a factor of two

greater than K_θ. In supplementary material we show an alternative model that gives $K_\theta^+/K_\theta \approx 1.5$. Because Eq. (12) uses experimental order parameters, it would seem that the ensuing tilt modulus should be compared to K_θ^+. However, all the corrections and approximations mentioned above for Eq. (12) would only decrease those values further, so there is an unresolved discrepancy regarding values of the thermodynamic tilt modulus K_θ^+.

Finally, x-ray data of the sort shown in Fig. 2 may provide another independent experimental measure of the same K_θ that appears in Eq. (9) if the analysis can be extended to include a tilt modulus. Alternatively, even if the low angle x-ray scattering data are insufficient to obtain K_θ independently, estimates of K_θ may help improve the fit to the low angle x-ray data and provide better values of K_C.

6. Discussion and Conclusions

Our group has found it very encouraging in the past that x-ray values of K_C agree so well with the MM values of (Rawicz et al., 2000). However, one has to consider that both sets of values may be artifactually too small. The reason that the x-ray values may be too small is that they are applied to data that are determined at a smaller length scale; in simulations, addition of a tilt degree of freedom increases the obtained value of K_C (May et al., 2007, Watson et al., 2012) and something similar might occur for the x-ray values. The reason that the MM values of (Rawicz et al., 2000) might be too small is that other studies have suggested that use of 200 mM sugar reduces K_C by a factor of two or more. Our new data show that glucose does not reduce the x-ray value of K_C. Our sucrose result also does not indicate a reduction, although more data should be obtained at higher concentration. Although the x-ray method does not yet include the tilt degree of freedom, nevertheless, it seems unlikely that a tilt dependent implementation would alter the observance or non-observance of a sugar effect.

It was recently suggested that the MM values of K_C may have been too small because the analysis did not include a tilt degree of freedom (Nagle, 2013). Importantly, we have here shown that adding a tilt degree of freedom is very unlikely to change either the MM or the SA values of K_C, so other causes must be hypothesized for the larger K_C values often obtained by the SA method compared to those obtained by the MM method. Nevertheless, it has been becoming increasingly clear that a tilt modulus K_θ, while secondary to the bending modulus K_C, is warranted in membrane mechanics, even though it is difficult to measure experimentally. This paper strengthens the case for including a tilt modulus by showing that several distinct approaches, theoretical models, simulations, and experimental order parameters obtain similar values of K_θ.

In conclusion, there are still unexplained differences in the experimental values of the bending modulus K_C, but the number of possible reasons has been reduced.

Supplementary Material

Refer to Web version on PubMed Central for supplementary material.

Acknowledgements

Bibliography

Andersen HD, Wang CH, Arleth L, Peters GH, Westh P. Reconciliation of opposing views on membrane-sugar interactions. Proceedings of the National Academy of Sciences of the United States of America. 2011; 108:1874–1878. [PubMed: 21245346]

Bouvrais, H. Bending Rigidities of Lipid Bilayers: Their Determination and Main Inputs in Biophysical Studies. In: Igli , A.; Genova, J., editors. Advances in Planar Lipid Bilayers and Liposomes. Academic Press; 2012.

Brandt EG, Braun AR, Sachs JN, Nagle JF, Edholm O. Interpretation of Fluctuation Spectra in Lipid Bilayer Simulations. Biophysical Journal. 2011; 100:2104–2111. [PubMed: 21539777]

Braun AR, Sachs JN, Nagle JF. Comparing Simulations of Lipid Bilayers to Scattering Data: The GROMOS 43A1-S3 Force Field. Journal of Physical Chemistry B. 2013; 117:5065–5072.

Dimova R. Recent developments in the field of bending rigidity measurements on membranes. Advances in Colloid and Interface Science. 2014 accepted.

Evans E, Rawicz W. Entropy-driven tension and bending elasticity in condensed-fluid membranes. Physical Review Letters. 1990; 64:2094–2097. [PubMed: 10041575]

Evans E, Rawicz W, Smith BA. Back to the future: mechanics and thermodynamics of lipid biomembranes. Faraday Discussions. 2013; 161:591–611. [PubMed: 23805759]

Genova J, Vitkova V, Bivas I. Registration and analysis of the shape fluctuations of nearly spherical lipid vesicles. Physical Review E. 2013; 88

Genova J, Zheliaskova A, Mitov MD. The influence of sucrose on the elasticity of SOPC lipid membrane studied by the analysis of thermally induced shape fluctuations. Colloids and Surfaces a-Physicochemical and Engineering Aspects. 2006; 282:420–422.

Genova J, Zheliaskova A, Mitov MD. Monosaccharides (fructose, glucose) and disaccharides (sucrose, trehalose) influence the elasticity of SOPC membranes. Journal of Optoelectronics and Advanced Materials. 2007; 9:427–430.

Genova J, Zheliaskova A, Mitov MD. Does maltose influence on the elasticity of SOPC membrane? Progress in solid state and molecular electronics, ionics and photonics, 2010. Institute of Physics. 012063(1–6)

Gracia RS, Bezlyepkina N, Knorr RL, Lipowsky R, Dimova R. Effect of cholesterol on the rigidity of saturated and unsaturated membranes: fluctuation and electrodeformation analysis of giant vesicles. Soft Matter. 2010; 6:1472–1482.

Hamm M, Kozlov MM. Tilt model of inverted amphiphilic mesophases. European Physical Journal B. 1998; 6:519–528.

Hamm M, Kozlov MM. Elastic energy of tilt and bending of fluid membranes. European Physical Journal E. 2000; 3:323–335.

Heinrich V, Waugh RE. A piconewton force transducer and its application to measurement of the bending stiffness of phospholipid membranes. Annals of Biomedical Engineering. 1996; 24:595–605. [PubMed: 8886240]

Helfrich W. Elastic Properties of Lipid Bilayers - Theory and Possible Experiments. Zeitschrift Fur Naturforschung C-a Journal of Biosciences, C. 1973; 28:693–703.

Henriksen JR, Ipsen JH. Thermal undulations of quasi-spherical vesicles stabilized by gravity. European Physical Journal E. 2002; 9:365–374.

Henriksen JR, Ipsen JH. Measurement of membrane elasticity by micro-pipette aspiration. European Physical Journal E. 2004; 14:149–167.

Khelashvili G, Harries D. How Cholesterol Tilt Modulates the Mechanical Properties of Saturated and Unsaturated Lipid Membranes. Journal of Physical Chemistry B. 2013; 117:2411–2421.

Koenig BW, Strey HH, Gawrisch K. Membrane lateral compressibility determined by NMR and X-ray diffraction: Effect of acyl chain polyunsaturation. Biophysical Journal. 1997; 73:1954–1966. [PubMed: 9336191]

Kucerka N, Nagle JF, Sachs JN, Feller SE, Pencer J, Jackson A, Katsaras J. Lipid bilayer structure determined by the simultaneous analysis of neutron and x-ray scattering data. Biophysical Journal. 2008; 95:2356–2367. [PubMed: 18502796]

Kucerka N, Tristram-Nagle S, Nagle JF. Structure of fully hydrated fluid phase lipid bilayers with monounsaturated chains. Journal of Membrane Biology. 2005; 208:193–202. [PubMed: 16604469]

Li DP, Hu SX, Li M. Full q-space analysis of X-ray scattering of multilamellar membranes at liquid-solid interfaces. Physical Review E. 2006; 73

Liu, Y-F. Dissertation. Carnegie Mellon University; 2003. New method to obtain structure of biomembranes using diffuse x-ray scattering: Application to fluid phase DOPC lipid bilayers; p. 1-128.http://lipid.phys.cmu.edu

Liu YF, Nagle JF. Diffuse scattering provides material parameters and electron density profiles of biomembranes. Physical Review E. 2004; 69

Lyatskaya Y, Liu YF, Tristram-Nagle S, Katsaras J, Nagle JF. Method for obtaining structure and interactions from oriented lipid bilayers. Physical Review E. 2001; 63

Marsh D. Elastic curvature constants of lipid monolayers and bilayers. Chemistry and Physics of Lipids. 2006; 144:146–159. [PubMed: 17045578]

May ER, Narang A, Kopelevich DI. Role of molecular tilt in thermal fluctuations of lipid membranes. Physical Review E. 2007; 76

May S, Kozlovsky Y, Ben-Shaul A, Kozlov MM. Tilt modulus of a lipid monolayer. Eur Phys J E Soft Matter. 2004; 14:299–308. [PubMed: 15338441]

Meleard P, Gerbeaud C, Bardusco P, Jeandaine N, Mitov MD, Fernandez-Puente L. Mechanical properties of model membranes studied from shape transformations of giant vesicles. Biochimie. 1998; 80:401–413. [PubMed: 9782381]

Meleard P, Gerbeaud C, Pott T, Fernandezpuente L, Bivas I, Mitov MD, Dufourcq J, Bothorel P. Bending elasticities of model membranes: Influences of temperature and sterol content. Biophysical Journal. 1997; 72:2616–2629. [PubMed: 9168037]

Mills TT, Toombes GES, Tristram-Nagle S, Smilgies DM, Feigenson GW, Nagle JF. Order parameters and areas in fluid-phase oriented lipid membranes using wide angle x-ray scattering. Biophysical Journal. 2008; 95:669–681. [PubMed: 18390624]

Nagle JF. Introductory Lecture: Basic quantities in model biomembranes. Faraday Discussions. 2013; 161

Nagle JF, Tristram-Nagle S. Structure of lipid bilayers. Biochimica Et Biophysica Acta-Reviews on Biomembranes. 2000; 1469:159–195.

Pan J, Tristram-Nagle S, Kucerka N, Nagle JF. Temperature dependence of structure, bending rigidity, and bilayer interactions of dioleoylphosphatidylcholine bilayers. Biophysical Journal. 2008; 94:117–124. [PubMed: 17827241]

Pan JJ, Tristram-Nagle S, Nagle JF. Effect of cholesterol on structural and mechanical properties of membranes depends on lipid chain saturation. Physical Review E. 2009; 80

Pecreaux J, Dobereiner HG, Prost J, Joanny JF, Bassereau P. Refined contour analysis of giant unilamellar vesicles. European Physical Journal E. 2004; 13:277–290.

Petersen NO, Chan SI. More on Motional State of Lipid Bilayer Membranes - Interpretation of Order Parameters Obtained from Nuclear Magnetic-Resonance Experiments. Biochemistry. 1977; 16:2657–2667. [PubMed: 889782]

Petrache HI, Gouliaev N, Tristram-Nagle S, Zhang RT, Suter RM, Nagle JF. Interbilayer interactions from high-resolution x-ray scattering. Physical Review E. 1998; 57:7014–7024.

Rawicz W, Olbrich KC, Mcintosh T, Needham D, Evans E. Effect of chain length and unsaturation on elasticity of lipid bilayers. Biophysical Journal. 2000; 79:328–339. [PubMed: 10866959]

Salditt T, Vogel M, Fenzl W. Thermal fluctuations and positional correlations in oriented lipid membranes. Physical Review Letters. 2003; 90

Seelig J, Seelig A. Lipid Conformation in Model Membranes and Biological-Membranes. Quarterly Reviews of Biophysics. 1980; 13:19–61. [PubMed: 7220788]

Shchelokovskyy P, Tristram-Nagle S, Dimova R. Effect of the HIV-1 fusion peptide on the mechanical properties and leaflet coupling of lipid bilayers. New Journal of Physics. 2011; 13

Sorre B, Callan-Jones A, Manneville JB, Nassoy P, Joanny JF, Prost J, Goud B, Bassereau P. Curvature-driven lipid sorting needs proximity to a demixing point and is aided by proteins. Proceedings of the National Academy of Sciences of the United States of America. 2009; 106:5622–5626. [PubMed: 19304798]

Sun WJ, Suter RM, Knewtson MA, Worthington CR, Tristram-Nagle S, Zhang R, Nagle JF. Order and Disorder in Fully Hydrated Unoriented Bilayers of Gel Phase Dipalmitoylphosphatidylcholine. Physical Review E. 1994; 49:4665–4676.

Tian AW, Capraro BR, Esposito C, Baumgart T. Bending Stiffness Depends on Curvature of Ternary Lipid Mixture Tubular Membranes. Biophysical Journal. 2009; 97:1636–1646. [PubMed: 19751668]

Tristram-Nagle, S. Preparation of Oriented, Fully Hydrated Lipid Samples for Structure Determination Using X-Ray Scattering. Totowa, NJ: Humana Press; 2007.

Vitkova V, Genova J, Mitov MD, Bivas I. Sugars in the aqueous phase change the mechanical properties of lipid mono- and bilayers. Molecular Crystals and Liquid Crystals. 2006; 449:95–106.

Vitkova, V.; Petrov, AG. Lipid bilayers and membranes: Material properties. In: Igli , A.; Genova, J., editors. Advances in Planar Lipid Bilayers and Liposomes. Academic Press; 2013.

Watson MC, Brandt EG, Welch AJ, Brown FLH. Determining biomembrane bending rigidities from simulations of modest size. Physical Review Letters. 2012; 109:4.

Watson MC, Morriss-Andrews A, Welch PM, Brown FLH. Thermal fluctuations in shape, thickness, and molecular orientation in lipid bilayers. II. Finite surface tensions. Journal of Chemical Physics. 2013; 139

Highlights

- Large uncertainties exist for values of the bending modulus of membranes

- The effect of sugar is considered, including new x-ray data

- Effect of tilt on data analysis is evaluated for different experimental methods
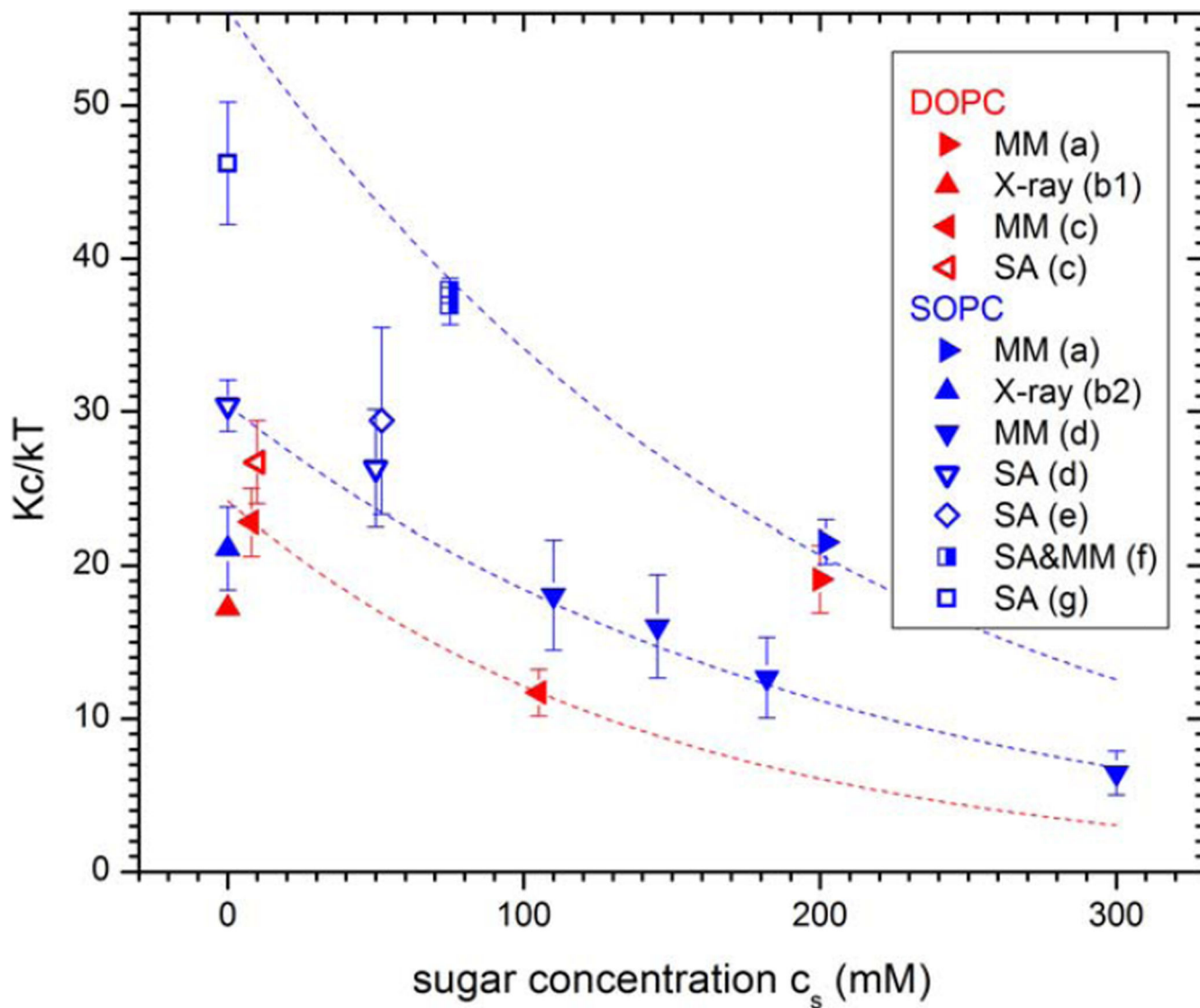
- Estimates of values of the tilt modulus are discussed

Figure 1.
Bending modulus K_C in thermal units kT versus sugar concentration c_s from literature values adjusted to T=30°C using −0.1/°C (Pan et al., 2008) for lipid bilayers composed of DOPC (downward pointing triangles) and SOPC (upward pointing triangles). The lines are exponential fits as proposed for SOPC (Vitkova et al., 2006). The legend identifies the method of measurement and the reference, a=(Rawicz et al., 2000), b1=(many results from this lab), b2=(Kucerka et al., 2005), c=(Shchelokovskyy et al., 2011), d=(Vitkova et al., 2006), e=(Pecreaux et al., 2004), f= (Henriksen and Ipsen, 2004), g=(Genova et al., 2013).
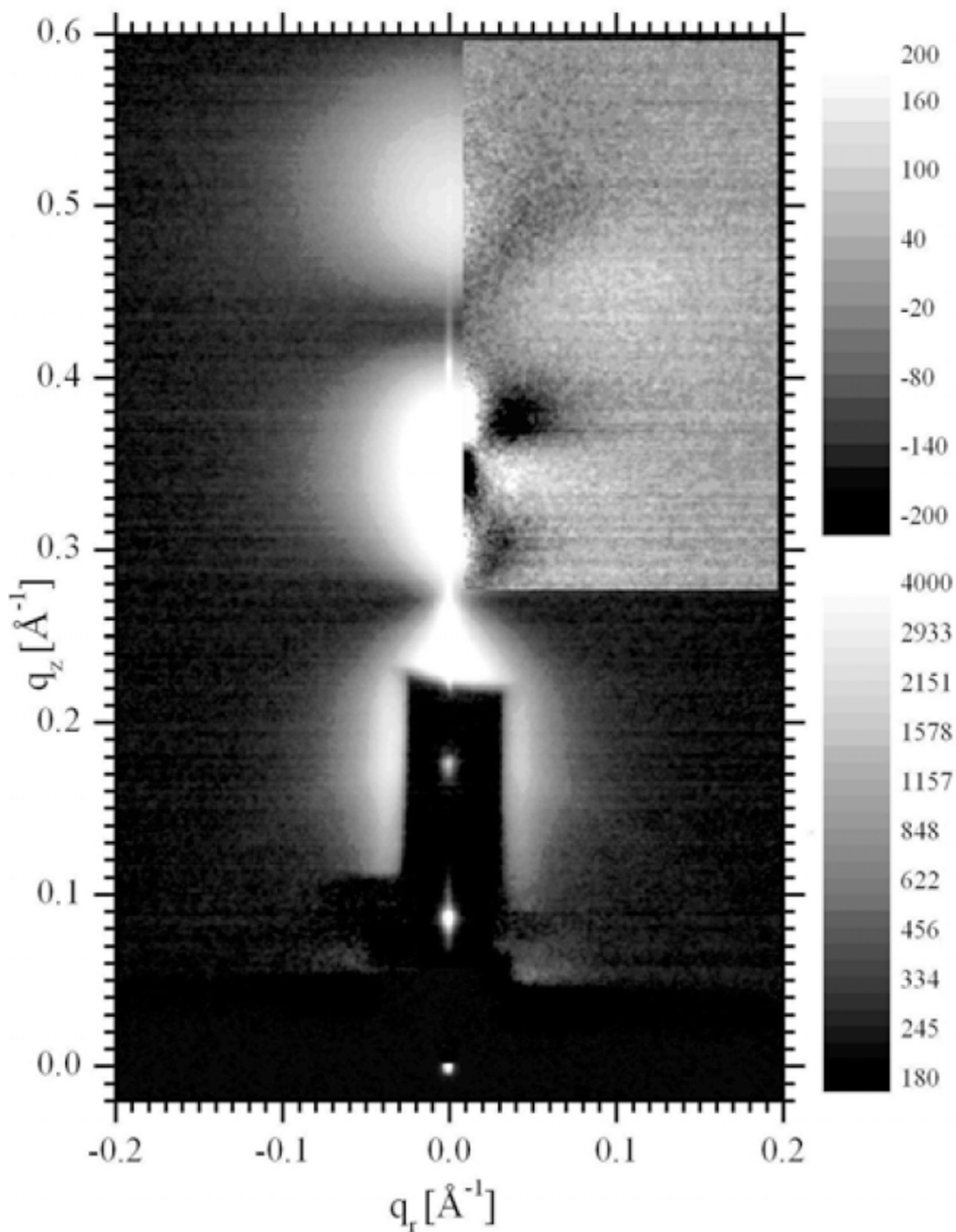
Figure 2.
X-ray scattering intensity from a stack of ~2000 oriented DOPC bilayers with glucose. The main panel shows the log of the intensity with the intensity scale shown at the lower right. The overlay in the upper right (positive q_r and $q_z > 0.28$ Å^{-1}) shows the residuals of the fit to the intensity in that region which is symmetrically equivalent to the intensity shown for negative q_r; the linear scale on the upper right shows that the residuals, though generally smaller than 2%, are non-random. A vertical molybdenum strip attenuates the h=1 and 2 orders on the meridian and a thicker horizontal strip attenuates the beam near the bottom.
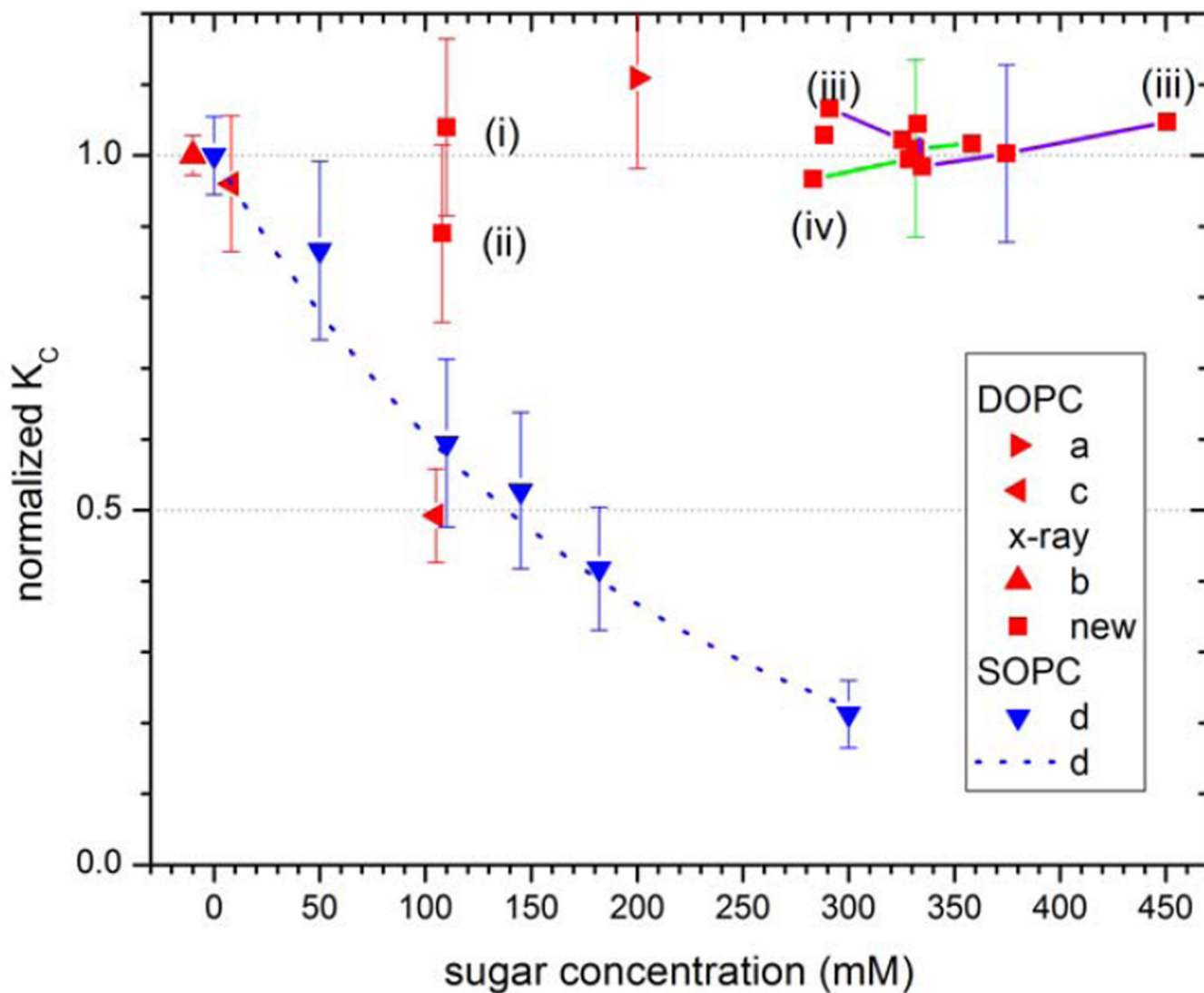
Figure 3.
Bending moduli normalized to 1 for zero sugar concentration. The dotted line is the exponential fit proposed for SOPC (Vitkova et al., 2006). The legend identifies the references, a=(Rawicz et al., 2000), b=(many results from this lab), c=(Shchelokovskyy et al., 2011),d=(Vitkova et al., 2006). The new x-ray data were obtained with glucose, samples (i), (iii) and (iv) and with sucrose, sample (ii). Estimated uncertainties for samples (iii) and (iv) should be applied to the average level of the purple and green lines, not to each concentration independently.
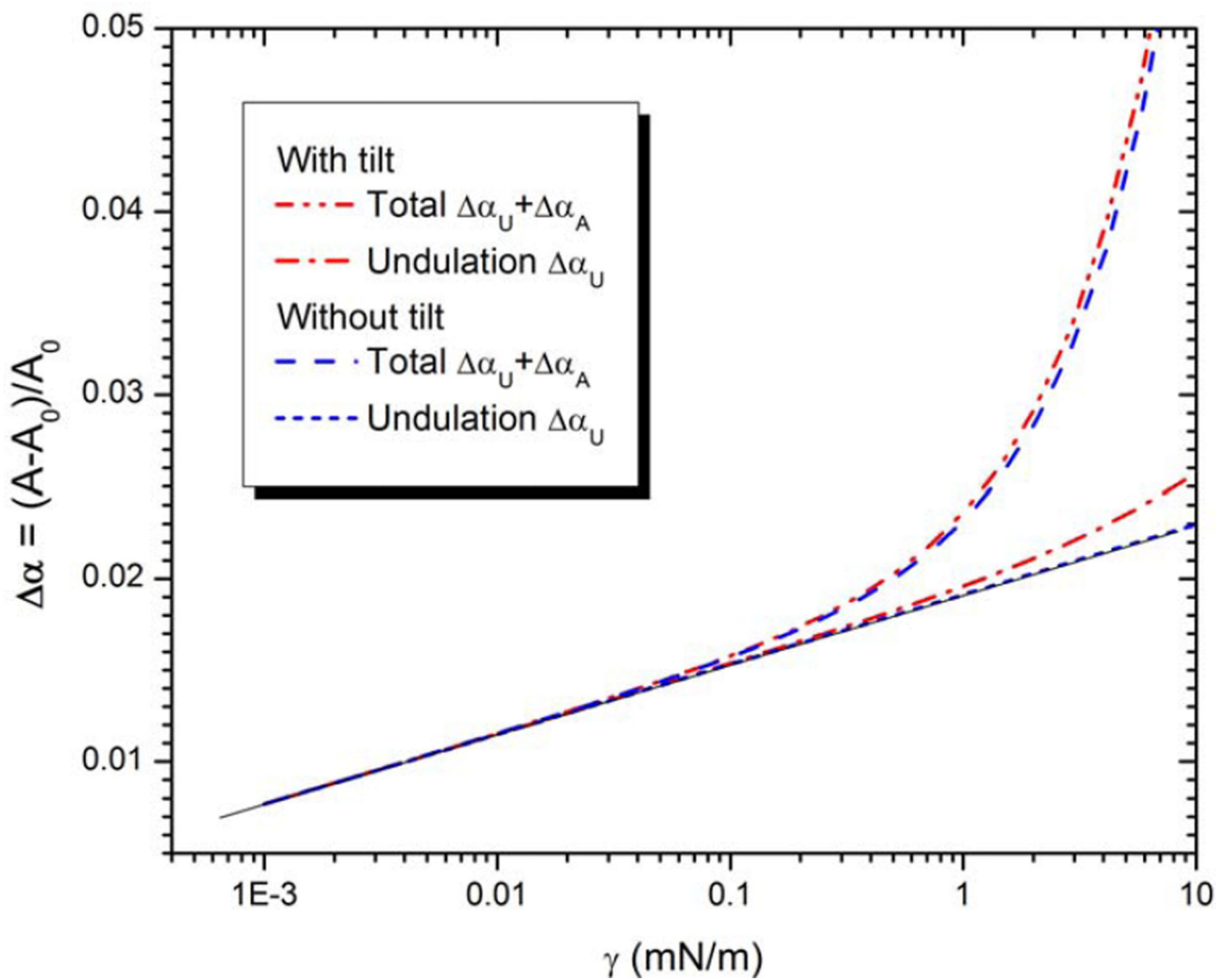
Figure 4.
Fractional area expansion α versus the log of the surface tension γ for the conventional model without tile and for the model with a tilt degree of freedom. The upper curves include direct expansion $\alpha_A = \gamma/K_A$ due to lateral compressibility with modulus K_A, and the lower curves show only the increase α_U due to undulations. Model parameters are $K_C = 10^{-19}$J, GUV radius R=10μm, molecular spacing a=0.8nm, K_A=250mN/m, K_θ=50mN/m for the theory with tilt and $K_\theta = \infty$ for the conventional theory. The thin black line has slope $kT/8\pi K_C$.
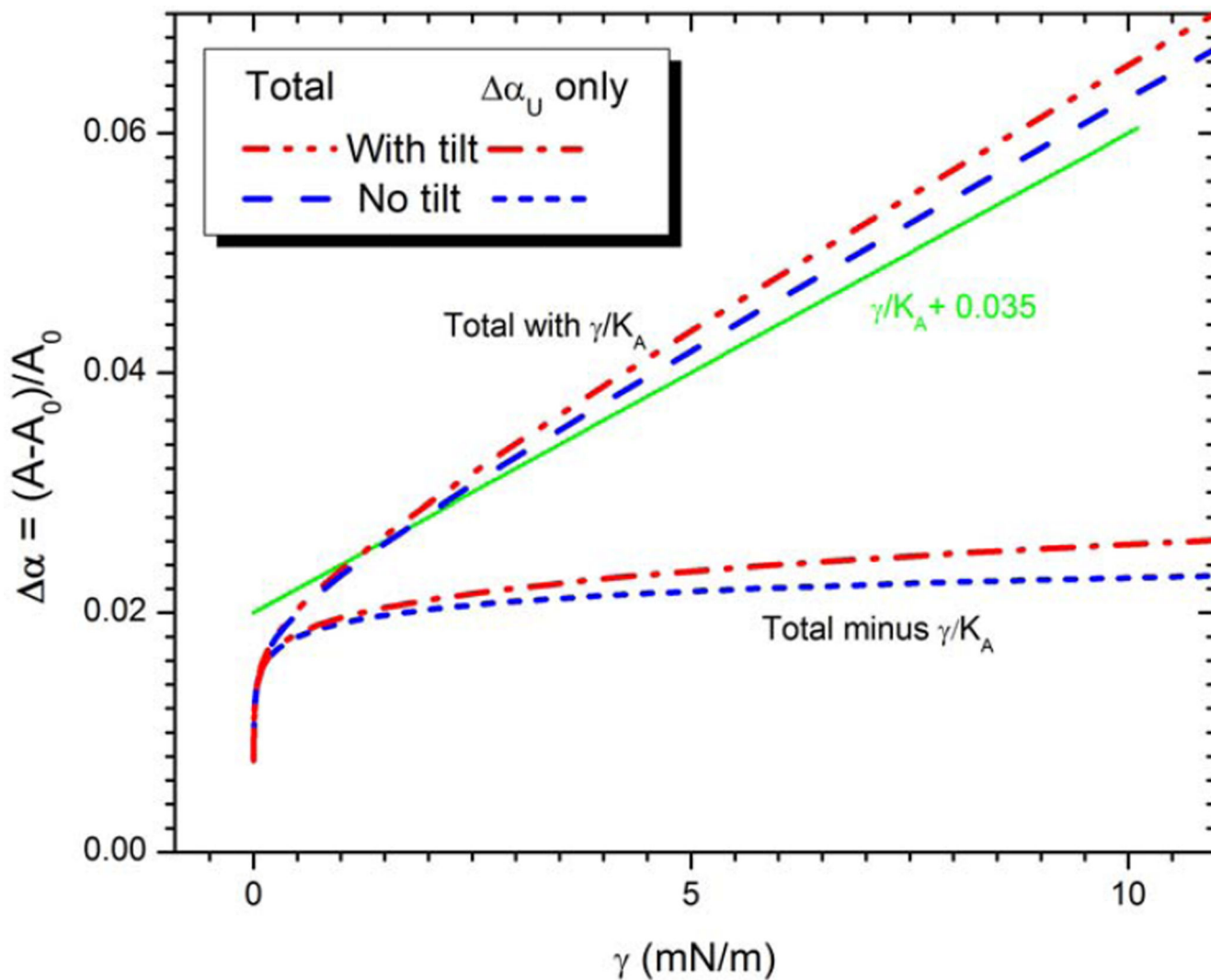
Figure 5.
Fractional area expansion α versus the surface tension γ for the conventional model with no tilt and for the model with a tilt degree of freedom. Similarly to Fig. 4, the upper curves show the total α and the lower curves show only the increase α_U just due to undulations. Model parameters are the same as in Fig. 4. The thin green line has slope equal to $1/K_A$.